

# Automatic Dimension Selection for a Non-negative Factorization Approach to Clustering Multiple Random Graphs

Nam H. Lee      I-Jeng Wang      Youngser Park  
Care E. Priebe      Michael Rosen

April 21, 2022

## Abstract

We consider a problem of grouping multiple graphs into several clusters using singular value thresholding and non-negative factorization. We derive a model selection information criterion to estimate the number of clusters. We demonstrate our approach using “Swimmer data set” as well as simulated data set, and compare its performance with two standard clustering algorithms.

## 1 Introduction

**Backgrounds** We consider an inference problem on a collection  $\mathcal{G}$  of  $T$  graphs where each graph  $G_t$  is a “histogram” of interaction events between  $n$  actors. In particular, for each  $t = 1, \dots, T$ , the  $(i, j)$ th entry  $G_{ij,t}$  of  $G_t$  encodes the number of times that person  $i$  and person  $j$  interacted during  $t$ th period. To describe our “graph clustering” problem, let  $(\kappa(1), G_1), \dots, (\kappa(T), G_T)$  be an (independent) sequence of pairs of a class label  $\kappa(t)$  and a graph  $G_t$ . We assume that the class label  $\kappa(t)$  takes values in  $\{1, \dots, r\}$  and also that given  $\kappa(t) = k$ ,  $G_t$  is a random graph on  $n$  vertices whose distribution depends only on the value of  $k$ . Our “graph clustering” problem is to estimate the value of  $r$ , and the value of  $\kappa(t)$  for each  $t = 1, \dots, T$  given the collection  $\mathcal{G} = \{G(1), \dots, G(T)\}$ .

To relate our problem to a non-negative factorization problem, denote by  $X$ , an  $n^2 \times T$  non-negative matrix such that for each  $t = 1, \dots, T$ , the  $t$ th column  $Xe_t$  of  $X$  is  $\text{vec}(G_t)$ . In words, each column of  $X$  is a vectorization of the non-negative integer valued adjacency matrix of each graph  $G_t$  with a fixed re-indexing rule. Specifically, we take  $X_{\ell,t} = G_{ij,t}$ , where  $\ell = n(j-1) + i$ , and we write  $Xe_t = \text{vec}(G_t)$ .

For our theoretical treatment later, we assume that each  $X_{\ell,t}$  is a Poisson random variable and the random variables  $(X_{\ell,t})$  are independent. We write  $\bar{X} := \mathbf{E}[X]$ .

**Definition 1.1.** The collection  $\mathcal{G}$  has  $r$  clusters provided that  $\bar{X} = \bar{W}\bar{H}\bar{\Lambda}$ , where  $\bar{W}$ ,  $\bar{H}$  and  $\bar{\Lambda}$  are  $n^2 \times r$ ,  $r \times T$  and  $T \times T$  full rank non-negative matrices such that  $\mathbf{1}^\top \bar{W} = \mathbf{1}^\top$ ,  $\mathbf{1}^\top \bar{H} = \mathbf{1}^\top$  and  $\bar{\Lambda}$  is a diagonal matrix.

Definition 1.1 amounts to a statement that  $\mathbf{E}[G_t] = \bar{\Lambda}_{tt} \sum_{k=1}^r \bar{Z}_k \bar{H}_{kt}$ , where  $\bar{Z}_k$  denotes the matrix that each  $\bar{Z}_{ij,k} := (\bar{W}e_k)_\ell$  with  $\ell = n(j-1) + i$ . As such, each  $\bar{\Lambda}_{tt}$  can be thought to be the interaction intensity for time  $t$ . As each  $\kappa(t)$  is to take values in  $\{1, \dots, r\}$ , we assume that each (column) vector  $\bar{H}_{\cdot t}$  is a standard basis in  $\mathbb{R}^r$ . Now, let  $N_t$  be the total weight on the edges of  $G_t$ , i.e.,  $N_t = \mathbf{1}^\top G_t \mathbf{1}$ , and we write  $\mathbf{N} = (N_1, \dots, N_T)$ . Let  $\boldsymbol{\mu}$  denote the matrix such that each column  $\boldsymbol{\mu}e_t = \text{vec}(G_t)/N_t$ . In our next definition, we use  $D(M|W, H)$  to denote a non-negative function of  $M, W, H$  that is typically used for a non-negative factorization algorithm. Some common choices of  $D$  includes  $\|M - WH\|_F$  and  $\|M - WH\|_1$ .

**Definition 1.2.** The optimal number  $r^*$  of cluster for the pair  $(\boldsymbol{\mu}, \mathbf{N})$  is the smallest positive integer  $r$  that minimizes

$$\text{AICc}(r) := \sum_{ij,t} (\widehat{W}^{(r)} \widehat{H}^{(r)})_{ij,t} \log((\widehat{W}^{(r)} \widehat{H}^{(r)})_{ij,t}) + \sum_{k=1}^r (\widehat{C}_k^{(r)} - 1) / \widehat{Q}_k^{(r)}, \quad (1)$$

where  $(\widehat{W}^{(r)}, \widehat{H}^{(r)})$  is such that  $D(\boldsymbol{\mu} : \widehat{W}^{(r)}, \widehat{H}^{(r)}) = \inf_{(W,H)} D(\boldsymbol{\mu}|W, H)$  with  $(W, H)$  ranging over ones such that  $\mathbf{1}^\top W = \mathbf{1}^\top \in \mathbb{R}^r$  and  $\mathbf{1}^\top H = \mathbf{1}^\top \in \mathbb{R}^T$ ,  $\widehat{Q}_k^{(r)} = \sum_{t=1}^T N_t \widehat{H}_{kt}^{(r)}$  and  $\widehat{C}_k^{(r)} = \sum_{ij} \mathbf{1}\{\widehat{W}_{ij,k}^{(r)} > 0\}$ .

Our nomenclature for ‘‘AICc’’ is motivated by the standard AIC formulation. Also, note that the value of  $r$  can be no less than but needs not be the rank of  $\bar{X}$ . To distinguish  $r$  from the rank of  $\bar{X}$ , we call  $r$  the *inner dimension* of  $\bar{X}$ . Although  $\bar{H}_{\cdot t}$  is assumed to be a column vector that is a standard basis in  $\mathbb{R}^r$ , we allow for the solution  $(\widehat{W}^{(r)}, \widehat{H}^{(r)})$  to be a probability vector other than a standard basis. As such, as a convention, given the optimal  $\widehat{r}$  and its associated  $(\widehat{W}^{(\widehat{r})}, \widehat{H}^{(\widehat{r})})$ , for each  $t$ , for our estimator  $\widehat{\kappa}(t)$  of  $\kappa(t)$ , we take  $\widehat{\kappa}(t)$  be such that  $\widehat{H}_{\widehat{\kappa}(t),t} \geq \widehat{H}_{k,t}$  for all  $k = 1, \dots, \widehat{r}$ .

**Related Works** Treating a sequence of graphs as a three way tensor, a non-negative tensor decomposition algorithm for the PARAFAC model can be applied in a way similar to our approach. For example, in [1], [2] and [3], by recording contact patterns using wearable sensors, a sequence of matrices is constructed, where each entry of a matrix records the number of near-proximity events between the wearable sensors, and subsequently, a metric called ‘‘core-consistency,’’ which was first introduced in [4], was used to determine the number of components for the non-negative tensor factorization. Alternatively, as in [5] and [6], one can consider each graph as a vector taking values in non-negative integers and then uses non-negative matrix factorization, and this is the approach that we also explore. In the classical model selection setting, e.g. for linear regression problems, information criteria approach is a popular choice,

(c.f. [7] and [8]) and we adopt this general strategy for our present setting. In [9], under some simplifying conditions, modeling the adjacency matrix of a random graph as a random matrix whose entries are Poisson random variables, it has been shown that such a random graph affords important statistical properties such as exchangeability, sparsity and power-law degree distribution, and this has motivated our distributional assumption on  $X$ . In [10] and [11], so-called “stochastic block model,” a general class of random graph model, is introduced and then, subsequently, studied for model estimation, and our simulation data is generated with a similar structural constraint.

## 2 Using an information criterion for determining the inner dimension

Our overall approach is a penalized maximum likelihood estimation. In particular, our derivation of the penalty term in the information criteria formula in Definition 1.1 is akin to the one in [8], in which for a linear regression problem, the penalty term is derived by computing the bias in the Kullback-Leibler discrepancy.

Our analysis in this section takes place in an asymptotic setting. Specifically, we consider a sequence of problems, where each problem is indexed by  $\ell$  so that for example, we have a sequence of collections of  $\mathcal{G}^{(\ell)}$ . The dependence of  $\mathcal{G}^{(\ell)}$  on  $\ell$  is only through Condition 1. Note that  $\bar{W}$  and  $\bar{H}$  do not depend on  $\ell$  even under Condition 1.

**Condition 1.** *Suppose that for each  $t$ , almost surely,*

$$\lim_{\ell \rightarrow \infty} N_t^{(\ell)} / \ell = \bar{\lambda}_t. \quad (2)$$

To simplify our notation, we suppress the dependence of our notation on  $\ell$  unless it is necessary. Also, with slight abuse of notation, for each  $k$ , we write  $\bar{\lambda}_k$  for the value of  $\bar{\lambda}_t$  for  $k(t) = k$ . Also, we let  $\bar{n}_k = |\{t : \kappa(t) = k\}|$ . The next condition states that the columns of  $\bar{W}$  are sufficiently different (c.f. [12]).

**Condition 2.** *The matrix  $\bar{W}$  is  $\nu$ -robust conical:*

$$\nu := \min_{i=1, \dots, r} \min_{\{h \in \mathbb{R}_+^r : h_i = 0\}} \|\bar{W}e_i - \bar{W}h\|_1 > 0. \quad (3)$$

Condition 3 is a stronger version of Condition 2, it amounts to a statement that the columns of  $\bar{W}$  have non-overlapping support. Moreover, after permuting the rows of  $\bar{W}$  if necessary, the matrix  $\bar{W}$  can be shown to have a block diagonal structure.

**Condition 3.** *For each  $1 \leq k_1 \leq k_2 \leq r$ ,*

$$e_{k_1}^\top \bar{W}^\top \bar{W} e_{k_2} = 0 \quad \text{if and only if} \quad k_1 \neq k_2. \quad (4)$$

**Lemma 2.1.** *Under Condition 1 and 2, there exists a non-negative factorization algorithm such that*

$$\lim_{\ell \rightarrow \infty} \|\widehat{W}^{(r)} - \overline{W}\|_F + \|\widehat{H}^{(r)} - \overline{H}\|_F = 0. \quad (5)$$

*Proof.* Note that by our assumption, the factorization  $\overline{W}\overline{H}$  is  $r$ -separable, i.e., the columns of  $\overline{H}$  form a basis for  $\mathbb{R}^r$  (c.f. [13] and [14]). Moreover, by assumption, we have  $\overline{W}$  is a  $\nu$ -robust conical with  $\nu > 0$ . Hence, we may choose our non-negative factorization algorithm to be the linear programming algorithm in [12]. On the other hand, as  $\ell \rightarrow \infty$ , we see that by a law of large numbers,  $\lim_{\ell \rightarrow \infty} X_{ij,t}/N_t = (\overline{W}\overline{H})_{ij,t}$  since  $\lim_{\ell \rightarrow \infty} N_t = \infty$ . Note that for each  $\varepsilon < \frac{\omega\kappa}{99(r+1)}$ , there exists  $\ell(\varepsilon) > 0$  such that for all  $\ell \geq \ell(\varepsilon)$ , with at least  $(1 - \varepsilon)$  probability,

$$\|X \text{diag}(\mathbf{1}^\top X)^{-1} - \overline{W}\overline{H}\|_1 \leq \varepsilon \quad (6)$$

where  $\omega = \min_{i \neq j} \|\overline{W}e_i - \overline{W}e_j\|_1$ . On such event, by Theorem 3 in [12], Algorithm 3 in [12] extracts  $(\widehat{W}, \widehat{H})$  such that

$$\|\overline{W} - \widehat{W}P\|_1 \leq 49(r+1)\frac{\varepsilon}{\nu} + 2\varepsilon. \quad (7)$$

for some permutation matrix of  $P$ . Since  $\varepsilon$  were arbitrary, this completes our proof for  $\widehat{W}^{(r)}$ .  $\square$

For our next observation, under a simplifying assumption, we examine the way that the first part of the penalty term of our AICc formula behaves. Specifically, fitting a model with a bigger number of clusters produces a bigger penalty term.

**Lemma 2.2.** *Suppose that  $(\widehat{W}, \widehat{H})$  is a non-negative factorization of  $\overline{W}\overline{H}$  with its inner dimension  $\widehat{r} > r$ , i.e.,  $\overline{W}\overline{H} = \widehat{W}\widehat{H}$  and also that  $\bar{\lambda}_k = 1$  for all  $k = 1, \dots, r$ . Under Condition 3, for each  $k = 1, \dots, r$ ,*

$$\sum_k \frac{\sum_{ij} \mathbf{1}\{\widehat{W}_{ij,k} > 0\}}{\bar{n}_k} \leq \sum_c \frac{\sum_{ij} \mathbf{1}\{\widehat{W}_{ij,c} > 0\}}{\widehat{n}_c}, \quad (8)$$

where  $\bar{n}_k = |\{t : \kappa(t) = k\}| = e_k^\top \overline{H}\mathbf{1}$  and  $\widehat{n}_c = e_c^\top \widehat{H}\mathbf{1}$ .

*Proof.* Since  $\overline{W}\overline{H}$  is  $r$ -separable, without loss of generality, to simplify our notation, we may assume that  $\overline{W} = \widehat{W}\widehat{H}$ , i.e., for each  $k = 1, \dots, r$ ,  $\overline{W}e_k = \widehat{W}\widehat{H}e_k$ . Now, by Condition 3,  $k_1 \neq k_2$  if and only if  $0 = e_{k_1}^\top \overline{W}^\top \overline{W}e_{k_2} = (\widehat{H}e_{k_1})^\top \widehat{W}^\top \widehat{W}(\widehat{H}e_{k_2})$ . Also, by permuting the rows and columns of  $\overline{W}$  if necessary, we may also assume, without loss of generality, that if  $k_1 < k_2$ , then

$$\max\{\ell : \overline{W}_{\ell, k_1}\} < \min\{\ell : \overline{W}_{\ell, k_2}\}. \quad (9)$$

For each  $k$ , let  $\mathcal{C}_k = \{c : \widehat{H}_{c,k} > 0\}$ . Then, together with the fact that  $\widehat{W}$  and  $\widehat{H}$  are non-negative matrices, one can show that the collection  $\{\mathcal{C}_k\}_{k=1}^r$  forms a partition of the set  $\{1, \dots, \widehat{r}\}$ , and also that by permuting the columns of  $\widehat{W}$  and the rows of  $\widehat{H}$  if necessary, for each  $k_1 < k_2$ ,

$$\begin{aligned} \max\{c : \widehat{H}_{c,k_1}\} &< \min\{c : \widehat{H}_{c,k_2}\}, \\ \max\{\ell : \widehat{W}_{\ell,r}, r \in k_1\} &< \min\{\ell : \widehat{W}_{\ell,r}, r \in k_2\}. \end{aligned}$$

Note that a significance of our last observation is that, roughly speaking, the non-zero entry structure of  $\widehat{W}$  and those of  $\widehat{H}$  match. To finish, fix  $k = 1, \dots, r$ . Then, since  $\overline{W}e_k = \sum_{c \in \mathcal{C}_k} \widehat{W}e_c$ , we must have, for each  $\ell$ , there exists  $c_{\ell,k} \in \mathcal{C}_k$  such that

$$\mathbf{1}\{\overline{W}_{\ell,k} > 0\} \leq \mathbf{1}\{\widehat{W}_{c_{\ell,k},k} > 0\}. \quad (10)$$

Hence,

$$\frac{\sum_{ij} \mathbf{1}\{\overline{W}_{ij,k} > 0\}}{\overline{n}_k} \leq \sum_{c \in \mathcal{C}_k} \frac{\sum_{ij} \mathbf{1}\{\widehat{W}_{ij,c} > 0\}}{\overline{n}_k} \leq \sum_{c \in \mathcal{C}_k} \frac{\sum_{ij} \mathbf{1}\{\widehat{W}_{ij,c} > 0\}}{\widehat{n}_c}, \quad (11)$$

where the last inequality follows because  $\overline{n}_k \geq \overline{n}_c$  for each  $c \in \mathcal{C}_k$  since for each  $t$ ,  $\overline{H}_{kt} \geq \widehat{H}_{ct}$ .  $\square$

For each  $t$ , note that  $Xe_t$  is a multinomial outcome from  $N_t$  independent trials and it constitutes a complete sufficient statistic for  $\overline{W}e_{\kappa(t)}$ . Hence, the data matrix  $X$  constitutes a complete and sufficient statistic for  $\overline{W}\overline{H}$ . In other words, our AICc is a function of a complete and sufficient statistic. If it is also unbiased, then by Lehman-Scheffe [15, Theorem 7.5.1], AICc would be an *uniformly minimum variance unbiased estimator* (UMVUE) of the (target) Kullback-Leibler discrepancy. Our next result shows that AICc is an unbiased estimator of  $\varphi(\overline{\mu})$  in the limit.

**Theorem 2.1.** *Under Condition 1,*

$$\lim_{\ell \rightarrow \infty} \ell \left( \mathbf{E}[\varphi(\widehat{W}, \widehat{H})] - \varphi(\overline{W}, \overline{H}) \right) = \sum_{k=1}^r \frac{\overline{C}_k - 1}{\overline{n}_k \overline{\lambda}_k}, \quad (12)$$

where the expectation is taken with respect to the parameter  $(\overline{W}, \overline{H}, \mathbf{N})$ ,  $\varphi(W, H) := \mathbf{E} \left[ \sum_{ij,t} (X_{ij,t}/N_t) \log((WH)_{ij,t}) \right]$  and  $\overline{C}_k = \sum_{ij} \mathbf{1}\{\overline{W}_{ij,k} > 0\}$ .

*Proof.* Write  $\widehat{\mu}_{ij,t} := X_{ij,t}/N_t$  and  $\widehat{C}_t = \sum_{ij} \mathbf{1}\{X_{ij,t} > 0\}$ . For any  $\widehat{W}$  and  $\widehat{H}$ , denoting  $\widehat{\mu} = \widehat{W}\widehat{H}$ , we have

$$\phi(\widehat{W}, \widehat{H}) = \sum_{ij,t} \mathbf{E}[X_{ij,t}]/N_t \log((\widehat{W}\widehat{H})_{ij,t}) = \sum_{ij,t} (\overline{W}\overline{H})_{ij,t} \log((\widehat{W}\widehat{H})_{ij,t}).$$

We now show that

$$\mathbf{E}[\varphi(\widehat{\mu})] = \varphi(\bar{\mu}) - \left( \sum_{t=1}^T \frac{\bar{C}_t - 1}{N_t} \right) + o_p(1).$$

To see this, note that by way of a Taylor expansion of the log function,

$$\varphi(\widehat{\mu}) = \phi(\bar{\mu}) + \mathbf{E} \left[ \sum_{ij,t} \bar{\mu}_{ij,t} \mathbf{1}\{\bar{\mu}_{ij,t} > 0\} \frac{1}{\bar{\mu}_{ij,t}} (\widehat{\mu}_{ij,t} - \bar{\mu}_{ij,t}) \right] \quad (13)$$

$$+ \mathbf{E} \left[ \sum_{ij,t} \bar{\mu}_{ij,t} \mathbf{1}\{\bar{\mu}_{ij,t} > 0\} \frac{-1}{\bar{\mu}_{ij,t}^2} (\widehat{\mu}_{ij,t} - \bar{\mu}_{ij,t})^2 \right] + o_p(1), \quad (14)$$

where  $o_p(1)$  is as  $\ell \rightarrow \infty$ . We will be more precise about the  $o_p(1)$  term in (14), but to simplify our analysis, we will appeal to the normal approximation of the binomial distribution. Specifically, rather than using the usual  $\varepsilon$ - $\delta$  argument, for simplicity, we choose to invoke the explicit form of the odd moments of a normal random variable. Now, we have, for all integers  $p > 0$ , if  $p$  is odd, then  $\mathbf{E}[(\widehat{\mu}_{ij,t} - \bar{\mu}_{ij,t})^p] = 0$ , and if  $p = 2\ell$  for some  $\ell \geq 1$ , then

$$\mathbf{E}[(\widehat{\mu}_{ij,t} - \bar{\mu}_{ij,t})^{2\ell}] = (\mathbf{E}[(\widehat{\mu}_{ij,t} - \bar{\mu}_{ij,t})^2])^\ell = \left( \frac{1}{N_t} \bar{\mu}_{ij,t} (1 - \bar{\mu}_{ij,t}) \right)^\ell.$$

Also,

$$\mathbf{E} \left[ \sum_{\ell=1}^{\infty} (\widehat{\mu}_{ij,t} - \bar{\mu}_{ij,t})^{2\ell} \right] = \sum_{\ell=1}^{\infty} \left( \frac{1}{N_t} \bar{\mu}_{ij,t} (1 - \bar{\mu}_{ij,t}) \right)^\ell = \left( \frac{1}{N_t} \bar{\mu}_{ij,t} (1 - \bar{\mu}_{ij,t}) \right) (1 + o_p(1)).$$

Since  $\widehat{\mu}$  is an unbiased estimator of  $\bar{\mu}$ , we see that the first term on the right in (13) vanishes to zero. For the second term in (14), we note that since each  $X_{ij,t}$  is a binomial random variable for  $N_t$  trials with its success probability  $\bar{\mu}_{ij,t}$ , we see that

$$- \sum_{ij,t} \mathbf{1}\{\bar{\mu}_{ij,t} > 0\} \frac{1}{\bar{\mu}_{ij,t}} \mathbf{E}[(\widehat{\mu}_{ij,t} - \bar{\mu}_{ij,t})^2] \quad (15)$$

$$= - \sum_{ij,t} \mathbf{1}\{\bar{\mu}_{ij,t} > 0\} \frac{1}{\bar{\mu}_{ij,t}} \frac{1}{N_t} \bar{\mu}_{ij,t} (1 - \bar{\mu}_{ij,t}) \quad (16)$$

$$= - \sum_{ij,t} \mathbf{1}\{\bar{\mu}_{ij,t} > 0\} \frac{1}{N_t} (1 - \bar{\mu}_{ij,t}) \quad (17)$$

$$= - \sum_{t=1}^T \frac{1}{N_t} \left( \sum_{ij} \mathbf{1}\{\bar{\mu}_{ij,t} > 0\} \right) + \sum_{t=1}^T \frac{1}{N_t} \left( \sum_{ij} \mathbf{1}\{\bar{\mu}_{ij,t} > 0\} \bar{\mu}_{ij,t} \right) \quad (18)$$

$$= - \sum_{t=1}^T \frac{\bar{C}_{\kappa(t)}}{N_t} + \sum_{t=1}^T \frac{1}{N_t}, \quad (19)$$

where the last equality is due to the fact that each column of  $\bar{\mu}$  sums to one. Hence, in summary, we see that

$$\lim_{\ell \rightarrow \infty} \ell(\mathbf{E}[\varphi(\widehat{W}, \widehat{H})] - \varphi(\overline{W}, \overline{H})) = - \lim_{\ell \rightarrow \infty} \ell \sum_{t=1}^T \frac{\overline{C}_t - 1}{N_t}. \quad (20)$$

Next, we note that in general,

$$\sum_{t=1}^T \frac{\overline{C}_t}{N_t} = \sum_{k=1}^r \sum_{t \in k} \frac{\overline{C}_t}{N_t} = \sum_{k=1}^r \overline{C}_{t_k} \sum_{t \in k} \frac{1}{N_t} = \sum_{k=1}^r \left( \frac{\overline{C}_{t_k}}{\sum_{t \in k} N_t} \left( \sum_{t \in k} \frac{1}{N_t / \sum_{s \in k} N_s} \right) \right),$$

where we write  $t \in k$  for  $\{t : \kappa(t) = k\}$  for simplicity. Then,

$$\lim_{\ell \rightarrow \infty} \sum_{t \in k} \frac{1}{N_t / \sum_{s \in k} N_s} = \lim_{\ell \rightarrow \infty} \sum_{t \in k} \frac{1}{(N_t/\ell) / \sum_{s \in k} (N_s/\ell)} = \sum_{t \in k} \frac{1}{\bar{\lambda}_t / \sum_{s \in k} \bar{\lambda}_s} = 1, \quad (21)$$

where the last equality is due to the fact that for each  $k$ ,  $\{G(t) : t \in k\}$  are identically distributed. Since  $\lim_{\ell \rightarrow \infty} \sum_{\kappa(t)=k} N_t/\ell = \bar{n}_k \bar{\lambda}_k$ ,

$$\lim_{\ell \rightarrow \infty} \ell \sum_{t=1}^T \frac{\overline{C}_t}{N_t} = \lim_{\ell \rightarrow \infty} \ell \sum_{k=1}^r \frac{\overline{C}_{t_k}}{\sum_{\kappa(t)=k} N_t} = \sum_{k=1}^r \frac{\overline{C}_{t_k}}{\lim_{\ell \rightarrow \infty} \sum_{\kappa(t)=k} N_t/\ell} = \sum_{k=1}^r \frac{\overline{C}_{t_k}}{\bar{n}_k \bar{\lambda}_k}. \quad (22)$$

Combining (20) and (22) completes our proof.  $\square$

## 2.1 On performing singular value thresholding

During our numerical experiments, we use the so-called singular value thresholding (SVT) as a variance reduction technique (c.f. [16]). We summarize our particular implementation of the technique. Specifically, assuming that  $X = U\Sigma V^\top$  is a singular value decomposition of  $X$  whose diagonal elements are non-increasing, we let  $\tilde{X} := U_+ \Sigma_+ V_+^\top$ , where  $U_+$  is the first  $\hat{r}$  columns of  $U$ ,  $V_+$  is the first  $\hat{r}$  columns of  $V$  and  $\Sigma_+$  is the top  $\hat{r} \times \hat{r}$  submatrix of  $\Sigma$ . Subsequently, since  $\widehat{X}$  may not be non-negative, we set each  $\widehat{X}_{ij}$  to be zero if  $\widehat{X}_{ij,t} < 0$ . Note that  $\widehat{X}$  may not be of rank  $\hat{r}$ . As such, we *iteratively* repeat the aforementioned procedure until the rank settles down to  $\hat{r}$ . In short, by virtue of Theorem 4.4 in [17, c.f. Section 3.2], one can see the singular value thresholding iteration specified above is related to the following optimization problem:  $\min_{Y \geq 0} \|Y - X\|_F^2$ , and also, the results in [16] can be used to show that a singular value thresholding can reduce the variance of the estimate. Roughly speaking, good performance of the technique is expected when the number of rows/columns is large. For more rigorous treatment of this technique, we direct the interested reader to [17] and [16]. Unless said otherwise, given a value for  $\hat{r}$ , during our numerical experiments, SVT at  $\hat{r}$  is used repeatedly until convergence, before running any NMF algorithm.

### 3 Numerical Experiments

**Computing environment** For non-negative factorization during our numerical experiments, we have used `nmf` function from the NMF package from R 3.0.1 (64-bit) under MAC OS X 10.9 on an Intel Core i5 @ 1.3 GHz machine with 4 GB RAM. Specifically, we use the option in `nmf` function that solves the following problem:

$$(\widehat{W}, \widehat{H}) := \arg \min_{W \geq 0, H \geq 0} \frac{1}{2} \|\overline{X} - WH\|_F^2 + \alpha \sum_{k_1 \neq k_2} e_{k_1}^\top W^\top W e_{k_2} + \beta \sum_{k,t} H_{k,t}, \quad (23)$$

where  $\mathbf{1}^\top W = \mathbf{1}^\top$  and  $\mathbf{1}^\top H = \mathbf{1}^\top$ , and  $\alpha, \beta \geq 0$  are chosen appropriately. A particular numerical algorithm solving the aforementioned problem for our experiment is known as *pattern-expression non-negative factorization* (c.f. [18]). Unless said otherwise, we use  $\alpha = 0$  and  $\beta = 1$ . Also, for the baseline algorithms for comparison, we use `pamk` and `Mclust` from the R packages `fpc` and `mclust` respectively for *partition around medoids* and *Gaussian mixture clustering* algorithms.

**Swimmer Data** The swimmer data set is a frequently-tested data set for bench-marking NMF algorithms (c.f. [19] and [12]). In our present notation, each column of  $220 \times 256$  data matrix  $X$  is a vectorization of a binary image, and each row corresponds to a particular pixel. Each image is a binary images (20-by-11 pixels) of a body with four limbs which can be each in four different positions. It is known that the matrix  $X$  is 16-separable while the rank of  $X$  is 13. Application of our AICc criteria using `nmf` with option `pe-nmf` with  $\alpha = 0$  and  $\beta = 1$  yields the estimated  $\hat{r}$  as 16 while using `nmf` with option `lee` yields  $\hat{r} = 18$ .

**Simulated Data** We now examine performance of our AICc criteria using simulated data. There are two parts to our Monte Carlo simulation analysis. First, we compare our algorithm against two other algorithms. Second, we examine whether or not performing singular value thresholding improves performance of our AICc criteria.

To begin, we specify the general set-up for our Monte Carlo experiments. For each  $t = 1, \dots, T$ , we generate  $G(t)$  as a weighted graph on  $n = 5 \times m$  vertices, where for each  $u, v = 1, 2, \dots, 5$ , the  $(u, v)$ th (non-overlapping) block  $G_{uv}(t)$  of  $G(t)$  is a weighted graph on  $m$  vertices. In particular, the  $(i, j)$ th entry of  $G_{uv}(t)$  is the  $(5(u-1) + i, 5(v-1) + j)$ th entry of  $G(t)$ .

Each block  $G_{uv}(t)$  is an random graph whose  $(i, j)$ th entry is an independent Poisson random variable with its expected value  $\overline{\Lambda}_{tt} \overline{B}_{uv}^{\kappa(t)}$ , where  $\kappa(t) \in \{1, 2\}$ . For our choice for  $\overline{B}_{uv}^{(k)}$ , we simplify the data from [20] in which ‘‘connectome’’ is constructed to answer a biological question, and obtain the following block

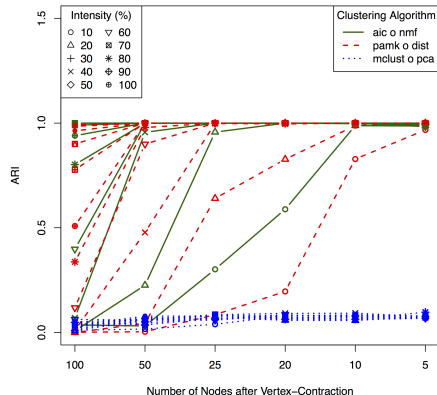


Figure 1: Comparison of three approaches through ARI for the model selection performance. The different symbols distinguish the different levels of intensity. The different line types distinguish the different algorithms. In all cases, our procedure either outperforms or nearly on par with the two baseline algorithms.

structured matrix:

$$\overline{B}^{(1)} := \begin{pmatrix} 0.1 & 0.045 & 0.015 & 0.19 & 0.001 \\ 0.045 & 0.05 & 0.035 & 0.14 & 0.03 \\ 0.015 & 0.035 & 0.08 & 0.105 & 0.04 \\ 0.19 & 0.14 & 0.105 & 0.29 & 0.13 \\ 0.001 & 0.03 & 0.04 & 0.13 & 0.09 \end{pmatrix}.$$

Then, we let  $\overline{B}^{(2)}$  to be the matrix obtained from  $\overline{B}^{(1)}$  by permuting the rows by the permutation (4152) and then by permuting the columns by the permutation (43). Our problem is then to estimate the number  $r$  of clusters using data  $G(1), \dots, G(T)$ , and the correct value for  $\hat{r}$  is  $r = 2$ . Before delving into our experiment results, we make some observation. First, as long as  $\overline{\Lambda}_{11} = \dots = \overline{\Lambda}_{TT} > 0$ , there should not be any statistically-significant evidence in the total number of edges in the graph that will distinguish one cluster from another. Next, viewing the sequence of graphs as a three-way tensor, one may fit a PARAFAC tensor model, but this can lead one to an unsatisfactory situation in which one has to disambiguate the relationship between the fact that  $\kappa(t)$  can take on two values and the rank of  $\overline{B}^{(k)}$  is 5.

For our first experimental result, we specify two other algorithms against which we compare our model selection procedure (AIC o nmf), where o denote composition of two algorithms. We denote our first baseline algorithm with (pamk o dist) and the second with (mclust o pca). For (pamk o dist), we first compute the distance/dissimilarity matrix using pair-wise Euclidean/Frobenius distances between graphs, and perform *partition around medoids* for clustering

(c.f. [21]). For (mclust o pca), we first compute the singular values of the data matrix  $X$  and use an “elbow-finding” algorithm to determine the rank of the data matrix (c.f. [7])

The experiment results are summarized in Figure 1. In all cases, our procedure either outperforms or nearly on par with the two baseline algorithms. There are two parameters that we varied, the level of intensity and the level of aggregation. For the level of intensity, for  $\rho \in (0, 1)$ , we take  $\bar{\Lambda}_t^{(\rho)} = \rho \bar{\Lambda}_t$ . For the level of aggregation (or equivalently, vertex-contraction), if the number of nodes after vertex-contraction is 5, the original graph is reduced to a graph with 5 vertices. Aggregation of edge weights is only done within the same block. Then, as the performance index, we use the adjusted Rand index (ARI) values (c.f. [22]).

Now, let us consider the performance of the algorithms with SVT and without SVT while we make the matrix sparser or denser by perturbing  $\bar{B}^{(1)}$  and  $\bar{B}^{(2)}$ . For each  $\varepsilon$ , two perturbation schemes are considered:

$$B^{(k)}(\varepsilon) = \left( \varepsilon \bar{B}^{(k)} \right), \quad (24)$$

$$B^{(k)}(\varepsilon) = \left( \bar{B}^{(k)} + \varepsilon \mathbf{1}\mathbf{1}^\top \right) \wedge \mathbf{1}\mathbf{1}^\top, \quad (25)$$

where  $\wedge$  denotes the component-wise minimum operator. We refer the clusters computed using SVT “implied” clusters, and the clusters computed without using SVT “apparent” clusters. When  $\varepsilon$  approaches 0,  $B^{(1)}(\varepsilon)$  approaches to the zero matrix while  $B^{(2)}(\varepsilon)$  approaches to itself. When  $\varepsilon$  approaches to 1,  $B^{(1)}(\varepsilon)$  approaches to itself while  $B^{(2)}(\varepsilon)$  approaches to  $\mathbf{1}\mathbf{1}^\top$ . Our experiment results are illustrated in Figure 2, and in summary, it demonstrates that using SVT widens the range of  $\varepsilon$  values for which, the correct value for  $r$  was obtained.

**Wearable Proximity Sensors in Hospital Wards** In [2], wearable sensors are used to detect close-range interactions between individuals in the geriatric unit of a university hospital. The study in [2] involves 46 health care workers and 29 patients over the span of 4 days and 4 nights. Individuals were grouped in four classes according to their role in the ward: patients (PAT), medical doctors (physicians and interns, MED), paramedical staff (nurses and nurses’ aides, NUR) and administrative staff (ADM). Grouping the actors by their roles (i.e., PAT, ADM, MED, NUR), we construct a collection of  $4 \times 4$  weighted adjacency matrices. Dividing the entire duration (4 days) to four intervals and then to twelve intervals, we arrive at two collections of  $4 \times 4$  weighted adjacency matrices. One can ask how the 12 period analysis compares with the 4 period analysis. For this, one can force on a 12 period the three cluster clustering, and search therein for a pattern consistent with the result from 4 period data whose optimal  $\hat{r} = 3$ . As reported in Table 1, the two clustering results are consistent with each other.

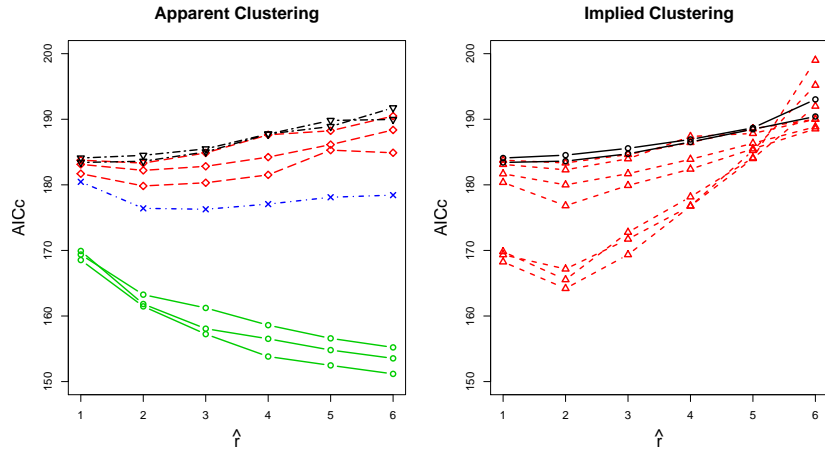
Table 1: How do fitting a three-cluster model on the daily version and on the 8-hour version correspond to each other? The letters A, B and C code three clusters for the daily version and the letters a, b and c code three clusters for the 8-hour version.

Num. of Graphs	Day 1	Day 2	Day 3	Day 4
4	A	B	C	C
12	(c,c,a)	(a,a,a)	(a,b,a)	(a,b,a)

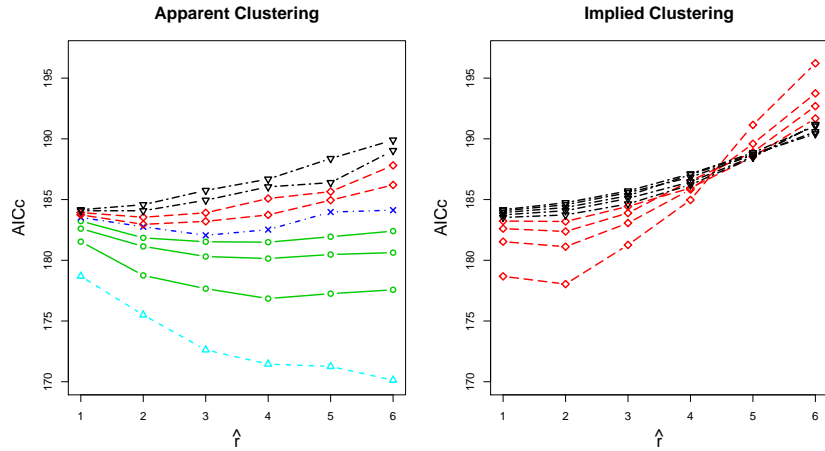
## References

- [1] A. Barrat, C. Cattuto, A. E. Tozzi, P. Vanhems, and N. Voirin, “Measuring contact patterns with wearable sensors: methods, data characteristics and applications to data-driven simulations of infectious diseases,” *Clinical Microbiology and Infection*, vol. 20, no. 1, pp. 10–16, 2014.
- [2] P. Vanhems, A. Barrat, C. Cattuto, J.-F. Pinton, N. Khanafer, C. Regis, B.-a. Kim, B. Comte, and N. Voirin, “Estimating potential infection transmission routes in hospital wards using wearable proximity sensors,” *PLoS ONE*, vol. 8, no. 9, p. e73970, 09 2013.
- [3] G. L. P. A. and C. C, “Detecting the community structure and activity patterns of temporal networks: A non-negative tensor factorization approach,” *PLoS ONE*, vol. 9, no. 1, 2014.
- [4] R. Bro and H. A. L. Kiers, “A new efficient method for determining the number of components in parafac models,” *Journal of Chemometrics*, vol. 17, pp. 274–286, 2003.
- [5] L. Hutchins, S. Murphy, P. Singh, and H. Graber, “Position-dependent motif characterization using non-negative matrix factorization,” *Bioinformatics*, vol. 24, no. 23, pp. 2684–2690, 2008.
- [6] J. Yang and J. Leskovec, “Overlapping community detection at scale: a nonnegative matrix factorization approach,” in *WSDM*, 2013, pp. 587–596.
- [7] M. Zhu and A. Ghodshi, “Automatic dimensionality selection from the scree plot via the use of profile likelihood,” *Computational Statistics & Data Analysis*, vol. 51, pp. 918–930.
- [8] S. L. Davies, A. A. Neath, and J. E. Cavanaugh, “Estimation optimality of corrected aic and modified  $c_p$  in linear regression,” *International Statistical Review*, vol. 74, no. 2, pp. 161–168, 2006.
- [9] F. Caron and E. Fox, “Bayesian nonparametric models of sparse and exchangeable random graphs,” 2014.

- [10] E. M. Airoldi, D. M. Blei, S. E. Fienberg, and E. P. Xing, “Mixed membership stochastic blockmodels,” *J. Mach. Learn. Res.*, vol. 9, pp. 1981–2014, Jun. 2008.
- [11] E. M. Airoldi, T. B. Costa, and S. H. Chan, “Stochastic blockmodel approximation of a graphon: Theory and consistent estimation,” in *Advances in Neural Information Processing Systems 26*, C. Burges, L. Bottou, M. Welling, Z. Ghahramani, and K. Weinberger, Eds. Curran Associates, Inc., 2013, pp. 692–700.
- [12] N. Gillis and R. Luce, “Robust near-separable nonnegative matrix factorization using linear optimization,” *Journal of Machine Learning Research*, pp. 1249–1280, 2014.
- [13] H. Laurberg, M. G. Christensen, M. D. Plumbley, L. K. Hansen, and S. H. Jensen, “Theorems on positive data: On the uniqueness of NMF,” *Computational Intelligence and Neuroscience*, vol. 2008, 2008.
- [14] K. Huang, N. D. Sidiropoulos, and A. Swami, “Non-negative matrix factorization revisited: Uniqueness and algorithm for symmetric decomposition,” *IEEE Transactions on Signal Processing*, vol. 62, no. 1, pp. 211–224, 2014.
- [15] G. Casella and R. Berger, *Statistical Inference*. Duxbury Resource Center, 2001.
- [16] R. H. Keshavan, A. Montanari, and S. Oh, “Matrix completion from noisy entries,” *The Journal of Machine Learning Research*, vol. 99, pp. 2057–2078, 2010.
- [17] J. Cai, E. Candes, and Z. Shen, “A singular value thresholding algorithm for matrix completion,” *SIAM Journal on Optimization*, vol. 20, no. 4, pp. 1956–1982, 2010.
- [18] J. Zhang, L. Wei, X. Feng, Z. Ma, and Y. Wang, “Pattern Expression Nonnegative Matrix Factorization: Algorithm and Applications to Blind Source Separation,” *Computational Intelligence and Neuroscience*, 2008.
- [19] D. Donoho and V. Stodden, “When does non-negative matrix factorization give correct decomposition into parts?” MIT Press, 2003, p. 2004.
- [20] E. M. Izhikevich and G. M. Edelman, “Large-scale model of mammalian thalamocortical systems,” *Proceedings of the National Academy of Sciences*, vol. 105, no. 9, pp. 3593–3598, 2008.
- [21] R. O. Duda and P. E. Hart, *Pattern Classification and Scene Analysis*. John Wiley & Sons, 1973.
- [22] W. Rand, “Objective criteria for the evaluation of clustering methods,” *Journal of the American Statistical Association*, 1971.



(a)  $B^{(k)}(\varepsilon)$  as in (24). More curves for “implied clustering” are minimized at  $\hat{r} = 2$ , i.e., 3 and 7 curves out of 9 are marked red resp. for apparent (Left) and implied (Right) clustering. As moving from the bottom curve to the top curve,  $\varepsilon$  assumes the values 0.8, 0.6, 0.4 and 0.2.



(b)  $B^{(k)}(\varepsilon)$  as in (25). More curves for “implied clustering” are minimized at  $\hat{r} = 2$ , i.e., 2 and 4 curves out of 9 are marked red resp. for apparent (Left) and implied (Right) clustering. As moving from the top curve to the bottom curve,  $\varepsilon$  assumes the values 0.8, 0.6, 0.4 and 0.2.

Figure 2: Different line colors (or equivalently, different line types for a black-and-white print) distinguish the different groups of values for  $\varepsilon$  according to the horizontal coordinate at which the AICc values for the curves are minimized. The correct value at which the curves should be minimized is  $r = 2$ . Black, red, blue, green and light blue are associated with the cases where the (estimated) number  $\hat{r}$  of clusters being 1, 2, 3, 4 and 5 respectively.